symmetry

MDPI

Article

Production of the Doubly Charged Higgs Boson in Association with the SM Gauge Bosons and/or Other HTM Scalars at Hadron Colliders

Bartosz Dziewit [1,*], Magdalena Kordiaczyńska [1] and Tripurari Srivastava [2]

[1] Institute of Physics, University of Silesia, 40-007 Katowice, Poland; mkordiaczynska@us.edu.pl
[2] Department of Physics, DIT University Dehradun, Uttarakhand 248009, India; tripurarisri022@gmail.com
* Correspondence: bartosz.dziewit@us.edu.pl

Abstract: We investigate an extension of the Standard Model with one additional triplet of scalar bosons. Altogether, the model contains four Higgs bosons. We analyze the associated production of the doubly charged scalar with the Standard Model gauge bosons and the remaining Higgs bosons of the model, which are: the light (SM) and heavy neutral scalars and a singly charged scalar. We estimate, in the context of the present (HL–LHC) and future (FCC–hh) hadron colliders, the most promising processes in which a single produced doubly charged Higgs boson is involved.

Keywords: theoretical physics; particle physics; Standard Model; Higgs triplets; doubly charged Higgs bosons; hadron colliders

Citation: Dziewit, B.; Kordiaczyńska, M.; Srivastava, T. Production of the Doubly Charged Higgs Boson in Association with the SM Gauge Bosons and/or Other HTM Scalars at Hadron Colliders. *Symmetry* **2021**, *13*, 1240. https://doi.org/10.3390/sym13071240

Academic Editors: Zoltán Trócsányi, Adam Kardos and Giuseppe Bevilacqua

Received: 11 May 2021
Accepted: 1 July 2021
Published: 10 July 2021

1. Introduction

Experimental evidence of the Higgs boson's existence, found at the Large Hadron Collider (LHC) [1,2], was a quantum leap in particle physics history. Nevertheless, questions related to the minimal Higgs sector are still open. From this point of view, extensions of the Standard Model can be realized in two ways: directly, by introducing additional multiplets, or indirectly, by extending the gauge group (e.g., left right symmetric models [3–8]). In the first scenario, many Beyond the Standard Model (BSM) theories assume the existence of additional Higgs bosons [9,10]. In the context of hadron colliders, doubly charged Higgs bosons [11–13] are especially attractive propositions; they lead to a production of same-charged leptons. In various BSM theories, they can occur at a significantly high rate. Thus, the Higgs sector with the Higgs triplet can lead to a discovery of new physics effects. In a general outline, triplet representations depend on the hypercharge $Y \equiv 2(Q - T_3)$ [13–16]. In this paper, we will focus on the Higgs Triplet Model (HTM), which extends the standard Higgs sector by adding one $SU(2)$ scalar triplet (Δ) with hypercharge $Y = 2$ [10,13]. The importance of investigation processes involving H^{++} is due to two facts. First, the triplet vacuum expectation value (VEV) is very small, whereas H^{++} mass can be at the level of a few hundred GeV. Such masses of H^{++} scalars can be probed at the hadron colliders. Second, processes involving H^{++} lead to the lepton flavor violation (LFV) as well as lepton number violating (LNV) processes, which can also be probed at hadron colliders. In addition, the model provides tiny masses of neutrinos by generating Majorana mass terms via the Type-II seesaw mechanism. Therefore, neutrino oscillation experiments put severe constraints on both the VEV v_Δ of the triplet scalar and Yukawa couplings.

The doubly charged Higgs bosons can be produced in pairs or as single events associated with gauge bosons and/or singly charged and neutral scalars. Amid the most important production channels at hadron colliders, it is worth mentioning the Drell-Yan processes via s-channel γ^*/Z^* or W^* exchange [17–19], the vector boson fusion process [20,21] or the gluon fusion process [22–24]. Pair production of doubly charged scalar and its signature as multi-leptons has been widely studied in the literature [25–38].

Searches of the charged scalars at the LHC show no significant excess from the SM backgrounds, thus lower bounds are put on their masses. The ATLAS collaboration set the lower bound on the mass of doubly charged scalar in the range of 770–870 GeV, assuming 100% branching ratios of leptonic modes [39] with $\sqrt{s} = 13$ TeV. Recently, ATLAS has searched the decay of doubly charged scalar into gauge bosons with multileptons in final states and established the lower bound on doubly charged scalar as 350 GeV (pair production) and 230 GeV [40]. The CMS collaboration has also provided lower bounds that vary between 396–712 GeV for a pair production (assuming 100% branching ratios of leptons) and 479–746 GeV for an associated production, depending on the decay channel bounds [41] with $\sqrt{s} = 13$ TeV. In this paper, we analyze the associated production of the doubly charged scalar with other scalars of the HTM model and/or SM gauge bosons. All relevant phenomenological constraints on the non-standard neutral and charged Higgs scalar parameters connected with HTM are taken into account. Among those worth mentioning are neutrino oscillations, low energy experiments, the bound on the ρ parameter, limits on HTM contributions to $(g-2)_\mu$ and lepton LFV processes, as well as limits on HTM parameters coming from collider e^+e^- and e^-e^- scatterings. We will present results obtained for HL–LHC $\sqrt{s} = 14$ TeV [42,43] and FCC-hh $\sqrt{s} = 100$ TeV [44–48] proton-proton collision energies.

2. The Higgs Triplet Model Phenomenological Constraints

To extend the Standard Model, one additional $SU(2)_L$ triplet Δ is introduced. Depending on the triplet hypercharge Y, this triplet contains neutral, singly and/or doubly charged scalar fields. In our case, since we are interested in the doubly charged Higgs production, we chose the $Y = 2$ and convention $Q = \frac{1}{2}Y + T_3$ (where T_3 is the third component of the izospin). So the scalar sector contains one doublet and the mentioned $Y = 2$ triplet:

$$\Phi = \frac{1}{\sqrt{2}}\begin{pmatrix} \sqrt{2}w_\Phi^+ \\ v_\Phi + h_\Phi + iz_\Phi \end{pmatrix}, \qquad \Delta = \frac{1}{\sqrt{2}}\begin{pmatrix} w_\Delta^+ & \sqrt{2}\delta^{++} \\ v_\Delta + h_\Delta + iz_\Delta & -w_\Delta^+ \end{pmatrix}. \tag{1}$$

The linear combination of neutral, charged and doubly charged fields of the above multiplets creates the physical states h (associated with the SM Higgs boson and mass around 125 GeV), H (heavy neutral boson), and singly $H^\pm$ and doubly charged $H^{\pm\pm}$ scalar particles (see Appendix A.1) and one pseudoscalar.

The entire Lagrangian can be found in [49] and is built from its kinetic potential and Yukawa parts. The scalar potential and the exact formulas for the scalar particles' masses can be found in the Appendix A.1.

In this work, we assume that the non-standard scalar particles' masses are degenerated. This choice is justified since the constraints from the unitarity, T-parameter and $h \to \gamma\gamma$ [50,51] process limit the mass gap between the M_H, $M_{H^\pm}$ and $M_{H^{\pm\pm}}$ to a few dozens of GeV [52,53].

Other constraints on the model parameters come from the low and high energy processes after the Yukawa part of the Lagrangian:

$$\mathcal{L}_Y^\Delta = \frac{1}{2} y_{\ell\ell'} L_\ell^T C^{-1} i\sigma_2 \Delta L_{\ell'} + \text{h.c.} \tag{2}$$

This leads to the $H^{\pm\pm} - l_i - l_j$ and $H^\pm - l_i - \nu_j$ vertices (see Appendix A.2). Therefore, this interaction provides contributions to several lepton flavor violating processes, for example, the $\ell_i \to \ell_j\gamma$, $\ell_i \to \ell_j\ell_k\ell_l$, $\mu \to e$ conversion. Besides, there are also contributions to a few standard model lepton scatterings and $(g-2)_\mu$ that are mediated by heavy charged scalars. These phenomenological constraints in the context of HTM have been analysed in detail in the literature [37]. Studies in [10,36,53,54] point out that $H^{\pm\pm}$ production strongly depends on neutrino oscillations, LHC and e^+e^- SM processes and low-energy lepton flavour violating data. It appears that the VEV of v_Δ is very small. Due to neutrino oscillation data, the v_Δ minimal value is constrained to be at the (sub)electronvolt level,

and due to theoretical constraints combined with low-energy neutral and charged processes, the v_Δ upper limit cannot exceed a gigaelectronovolt value. In this work, we take $v_\Delta = 50$ eV and $v_\Delta = 0.5$ GeV as reference values.

3. Results

Let us first analyse the production $2 \to 2$ and $2 \to 3$ processes at hadron colliders where a single $H^{\pm\pm}$ boson and SM gauge bosons or other Higgs scalars of the HTM model are simultaneously produced. We use the CTEQ6L1 Parton Distribution Functions (PDF) [55,56] and basic MadGraph cuts. In Table 1, we present production rates for eleven non-vanishing processes. Other processes with two neutral bosons production, such as, for example, $pp \to H^{\pm\pm}Zh$, are forbidden by the charge conservation principle. For the reader's convenience, the most promising processes are given in blue. Corresponding Feynman diagrams, which contribute to the processes shown in Table 1, are presented in the Appendix A.3. In this work, calculations have been performed using the MadGraph [57] and Pythia [58,59] programs. The UFO files were generated using FeynRules [60] and were built on our model file [37,53,61], based on the default Standard Model implementation.

The dominant process associated with a single $H^{\pm\pm}$ production is $pp \to H^{\pm\pm}H^{\mp}$. The expected cross sections for the given Higgs boson masses are 8.13×10^{-5} for $\sqrt{s} = 14$ TeV, and 8.78×10^{-3} pb for $\sqrt{s} = 100$ TeV. With assumed luminosity $L = 4\ ab^{-1} = 4000\ fb^{-1}$ for HL–LHC [43] and $L = 25\ ab^{-1} = 25000\ fb^{-1}$ for FCC–hh [47], it converts to a total number of $\sim$300 and $\sim 2 \times 10^5$ events at HL–LHC and FCC–hh, respectively.

The following 'blue' processes in Table 1 are connected with $2 \to 3$ processes. The processes that provide negligible cross sections can be understood by analysing individual Feynman vertices; see the Appendix A.3 and Table 2. As we can see in Table 2, many vertices are proportional to VEV v_Δ, which, as explained in Sections 1 and 2, is at the level of (sub)eV-GeV.

Table 1. Cross section for a production of a single $H^{\pm\pm}$ boson with associated SM gauge bosons and other HTM scalars at the pp colliders in $2 \to 2$ and $2 \to 3$ processes. Cross sections are calculated for $\sqrt{s} = 14$ TeV (100 TeV) and are given in pb. Charged scalar masses are degenerated, $M_{H^{\pm\pm}} = M_{H^{\pm}} = 1000$ GeV.

	Process	Cross Section [pb]		Process	Cross Section [pb]
(I)	$pp \to H^{\pm\pm}W^{\mp}$	$\sim 10^{-22}$ ($\sim 10^{-20}$)	(II)	$pp \to H^{\pm\pm}H^{\mp}$	8.13×10^{-5} (8.78×10^{-3})
(III)	$pp \to H^{\pm\pm}ZW^{\mp}$	$\sim 10^{-12}$ (2.7×10^{-9})	(IV)	$pp \to H^{\pm\pm}ZH^{\mp}$	6.29×10^{-7} (1.56×10^{-4})
(V)	$pp \to H^{\pm\pm}W^{\mp}W^{\mp}$	$\sim 10^{-10}$ (1.87×10^{-9})	(VI)	$pp \to H^{\pm\pm}W^{\mp}h$	$\sim 10^{-12}$ (3.47×10^{-8})
(VII)	$pp \to H^{\pm\pm}W^{\mp}H$	1.35×10^{-6} (2.44×10^{-4})	$(VIII)$	$pp \to H^{\pm\pm}W^{\mp}H^{\mp}$	2.88×10^{-6} (6.81×10^{-4})
(IX)	$pp \to H^{\pm\pm}hH^{\mp}$	1.07×10^{-7}) (1.63×10^{-6}	(X)	$pp \to H^{\pm\pm}HH^{\mp}$	$\sim 10^{-29}$ ($\sim 10^{-26}$)
(XI)	$pp \to H^{\pm\pm}H^{\mp}H^{\mp}$	$\sim 10^{-31}$ ($\sim 10^{-28}$)			

Table 2. Couplings for the non standard scalars: $H^{\pm}$ (charged, top table) and H (neutral, bottom table).

Decay Channel	Coupling	Decay Channel	Coupling	Decay Channel	Coupling
$H^{\pm} \to W^{\pm}\, h$	$\sim v_{\Delta}$	$H^{\pm} \to W^{\pm}\, \gamma$	$\sim v_{\Delta}$	$H^{\pm} \to W^{\pm}\, Z$	$\sim v_{\Delta}$
$H^{+} \to l_i^{+}\, \bar{\nu}_j$	$\sim y_{\ell_i \ell_j} \sim \frac{1}{v_{\Delta}}$	$H^{+} \to l_i^{+}\, \nu_j$	$\sim \frac{v_{\Delta}}{v_{\Phi}}$	$H^{\pm} \to q_i \bar{q}_j$	$\sim \frac{\sqrt{2}}{v_{\phi}} CKM$
$H \to h\, h$	$\sim v_{\Delta}$	$H \to W^{+}\, W^{-}$	$\sim v_{\Delta}$	$H \to Z\, Z$	$\sim v_{\Delta}$
$H \to l^{+}\, l^{-}$	$\sim v_{\Delta}$	$H \to q\, \bar{q}$	$\sim v_{\Delta}$		

In Figure 1, the $M_{H^{\pm\pm}}$ mass dependence of the $pp \to H^{\pm\pm} H^{\mp}$ cross section is given. As we can see, it depends strongly on the doubly charged Higgs boson mass. Note that in Table 1, results are given for $M_{H^{\pm\pm}} = M_{H^{\pm}} = 1000$ GeV. However, as discussed in the Introduction and in [37], smaller masses of heavy Higgs bosons are still possible, so signal predictions given for processes in Table 1 can be even larger.

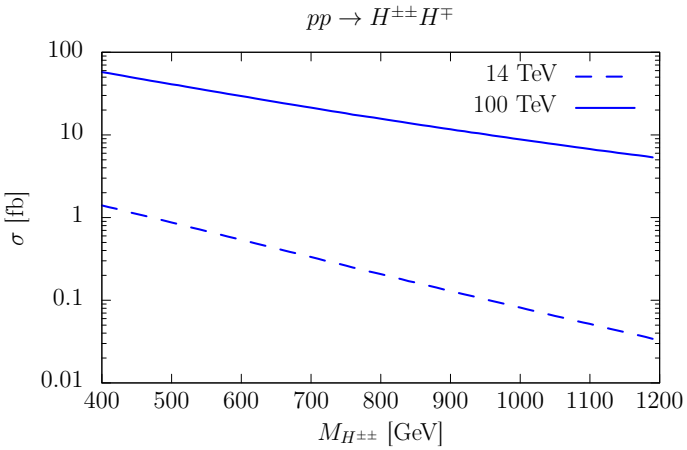

Figure 1. Cross section for $pp \to H^{\pm\pm} H^{\mp}$ process as a function of $M_{H^{\pm\pm}}$. In the calculations, $M_{H^{\pm}}$ is taken to be 1000 GeV.

Concerning the decay modes of the HTM Higgs bosons, in the case of doubly charged Higgs boson $H^{\pm\pm}$, we discussed the decay channels in detail in Section 5.2 of our previous work [37]. Here, we initiate a similar analysis for singly charged $H^{\pm}$ and heavy neutral scalar bosons H. First, possible decay modes of $H^{\pm}$ and H with corresponding strengths of interactions (couplings) are given in Table 2.

As one can find in Table 2, singly charged scalar $H^{\pm}$ coupling can break the lepton number ($H^{+} \to l_i^{+} \nu_j$) and lepton flavour number ($H^{+} \to l_i^{+} \tilde{\nu}_j$). These couplings also contribute to muon $(g-2)_{\mu}$, which was discussed in the Appendix of [37].

As we mentioned in Section 2, the triplet VEV v_{Δ} is bounded from below due to the LFV processes and from the top because of the ρ parameter constrain. From Table 2 we can see that $H^{\pm}$ decay depends on v_{Δ}, as well as the doubly charged scalar decay modes (see Figure 11 in [37]). Due to the assumed scalar's mass degeneration, decays to the non-standard scalars are not considered, even though those might be significant as off-shell processes and are worth discussion in future studies.

Since $H^{\pm\pm}$ and $H^{\pm}$ decays depend on the triplet VEV, to examine different decay modes, we choose two values; v_{Δ} = 50 eV and v_{Δ} =0.5 GeV. We assume degenerated mass scenario $M_{H^{\pm\pm}} = M_{H^{\pm}} = M_H$. For v_{Δ} = 50 eV, the doubly charged scalar $H^{\pm\pm}$ decays dominantly to a pair of leptons, and $H^{\pm}$ decays to a charged lepton and an (anti)neutrino. Branching ratios for particular flavours depend on the neutrino mass hierarchy and mixing angles. In the second case, $v_{\Delta} = 0.5$ GeV, $H^{\pm\pm}$ decays to a gauge boson pair $W^{\pm} W^{\pm}$. Regarding the singly charged scalar $H^{\pm}$, the situation is a bit more complicated as shown in Figure 2. For clarity, we present the dominant decay channels for $H^{\pm\pm}$ and $H^{\pm}$ in Table 3. Other possible final states are negligible.

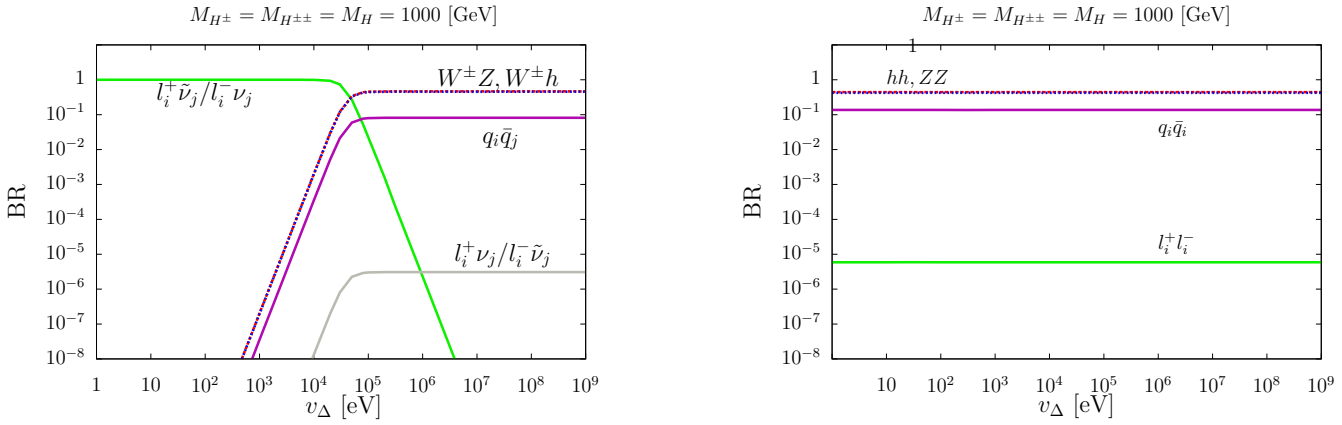

(**a**) (**b**)

Figure 2. Branching ratios for $H^\pm$ (charged, **a**) and H (neutral, **b**) Higgs boson decays in `HTM`.

Table 3. Dominant decays of $H^\pm$ and $H^{\pm\pm}$ for different values of triplet VEV, v_Δ = 50 eV and v_Δ = 0.5 GeV.

v_Δ = 50 eV	$H^\pm$	$\rightarrow$	$l_i^-\,\nu_j$ / $l_i^+\,\tilde{\nu}_j$	$H^{\pm\pm}$	$\rightarrow$	$l_i^\pm\,l_j^\pm$
v_Δ = 0.5 GeV	$H^\pm$	$\rightarrow$	$W^\pm\,Z$ $W^\pm\,h$ $q_i\,\bar{q}_j$	$H^{\pm\pm}$	$\rightarrow$	$W^\pm\,W^\pm$

The final state for the above processes depends on the SM and heavy scalar particles' decays. For the purpose of this work, we chose the least complicated case—the $pp \rightarrow H^{\pm\pm}H^\mp$ process. As one can see in Table 3, decay modes depend on the triplet VEV. Moreover, in the same table we presented the simplified relationship between the scalar-leptons couplings and triplet and doublet VEVs. In the Table 4 we present the cross section for the intermediate states and corresponding background. In the Appendix A.2, we demonstrate more exact formulas. Those vertices depend on the PMNS matrix—on neutrino mixing parameters and mass hierarchy. Because decay to a $l_i^\pm l_j^\pm$ pair depends strongly on the neutrino parameters, we decided to follow the convention adopted in [37] and find the parameter space where decay to same flavour lepton is most probable. That means:

- to maximize the $e^\pm\,e^\pm\,e^\mp$ signal: $m_{\nu_3} = 0$ (inverted neutrino mass hierarchy), $\alpha_1 = \frac{\pi}{2}$, $\alpha_2 = \frac{\pi}{2}$,
- to maximize the $\mu^\pm\mu^\pm\mu^\mp$ signal: $m_{\nu_1} = 0.015$ eV (normal neutrino mass hierarchy), $\alpha_1 = 0$, $\alpha_2 = 0$,

where α_1, α_2 are Majorana phases in the PMNS matrix (see Equation (A9)) and other neutrino parameters are taken from nu-fit.org (accessed on 2 July 2021) [62].

Table 4. Singly and doubly charged scalar production $pp \to H^{\pm\pm}H^{\mp}$ with primary decays to the SM particles for CM energy 14 TeV (100 TeV).

v_Δ	Process:			Signal [pb]:	Background [pb]:
50 eV	$pp \to H^{\pm\pm}H^{\mp}$	$\to$	$e^{\pm}\, e^{\pm}\, e^{\mp}\, \not{E}_T$	1.79×10^{-5} (2.00×10^{-3})	5.05×10^{-2} (3.15×10^{-1})
			$\mu^{\pm}\mu^{\pm}\mu^{\mp}\, \not{E}_T$	1.43×10^{-5} (1.55×10^{-3})	5.05×10^{-2} (3.15×10^{-1})
0.5 GeV	$pp \to H^{\pm\pm}H^{\mp}$	$\to$	$W^{\pm}W^{\pm}W^{\mp}\, Z$	3.62×10^{-5} (3.93×10^{-3})	7.00×10^{-4} (1.60×10^{-2})
			$W^{\pm}W^{\pm}W^{\mp}h$	3.53×10^{-5} (3.84×10^{-3})	6.19×10^{-5} (1.12×10^{-3})
			$W^{\pm}W^{\pm}jj$	3.68×10^{-10} (4.01×10^{-8})	3.09×10^{-1} (5.65)

In Table 4, we present the above process with primary scalar particles and Standard Model particles. As one can see, for $v_\Delta = 50$ eV, the possible final state is $l^{\pm}l^{\pm}l^{\mp}\not{E}_T$. In Table 5, we present the results after using the following cuts:

- Lepton identification criteria: transverse momentum $p_T \geq 20$ GeV, pseudorapidity $|\eta| < 2.5$;
- Hard p_T cuts: $p_T(l_1) > 30$ GeV, $p_T(l_2) > 30$ GeV, $p_T(l_3) > 20$ GeV;
- Detector efficiency for electron (muon): 70% (90%);
- Lepton–lepton separation: $\Delta R_{ll} \geq 0.2$;
- Z-veto—the invariant mass of any same flavour and opposite charge lepton should satisfy the condition: $|m_{l_1 l_2} - M_{Z_1}| \geq 6\,\Gamma_{Z_1}$.

The signal after the above cuts for $v_\Delta = 50$ eV is still negligible in comparison to the background. However, we are planning to repeat the above studies for 0.5 GeV, since that case looks much more promising.

Table 5. Results from Table 4 for $v_\Delta = 50$ eV, after cuts. Centre mass energy: $\sqrt{s} = 14$ TeV.

Process:	Signal:		Background:	
	Before Cuts [pb]:	After Cuts [fb]:	Before Cuts [pb]:	After Cuts [fb]:
$e^{\pm}\, e^{\pm}\, e^{\mp}\ \not{E}_T$	1.79×10^{-5}	5.46×10^{-3}	5.05×10^{-2}	0.94
$\mu^{\pm}\, \mu^{\pm}\, \mu^{\mp}\, \not{E}_T$	1.43×10^{-5}	9.68×10^{-3}	5.05×10^{-2}	1.77

4. Summary and Outlook

Observation of the Higgs boson opens up possibilities for other charged and neutral scalars to be detected at present and future colliders. In this paper, we studied the associated production of a doubly charged scalar within the Higgs triplet model at the pp colliders and with a centre of mass energy of 14 (HL–LHC) and 100 TeV (FCC–hh). We analysed all the associated processes of $H^{\pm\pm}$ with gauge and scalar bosons and found that five of them are worth further study. We found that the largest cross section is for the $pp \to H^{\pm\pm}H^{\pm}$ process. Our preliminary studies show that the background signals for the considered processes are substantial, and a more detailed analysis of kinematic conditions and appropriate distributions or choice of final states, which can enhance new physics signals over the SM background, are needed and will be undertaken in the near future.

Further, we analyzed the dominant decay modes of singly charged and heavy neutral scalars within the model. The final state's signature at the hadron colliders will depend strongly on HTM VEV; we discuss possible decay scenarios for $v_\Delta = 50$ eV and $v_\Delta = 0.5$ GeV. For $v_\Delta = 50$ eV, the dominant decay modes are leptonic, while for $v_\Delta = 0.5$ GeV the

dominant modes involve SM gauge bosons. Scenarios with off-shell, non-standard scalar decays will also be compelling to explore.

We have examined the $v_\Delta = 50$ eV. Even though applied cuts slightly improved the significance, the result is still very low compared to the background. We are planning to repeat the detailed studies with appropriate cuts for $v_\Delta = 0.5$ GeV, which seems to be more attractive in comparison to the background.

As an outlook similar to the work in [37], for a case of doubly charged Higgs boson pair production at hadron colliders, we should consider how HTM signals—where a single $H^{\pm\pm}$ Higgs boson is involved—can be discriminated from other models, including $H^{\pm\pm}$ scalars, notably the Left–Right Symmetric Models [21,52,63–66].

Author Contributions: Conceptualization, M.K.; methodology, B.D., M.K. and T.S.; software, B.D. and M.K.; validation, B.D. and T.S.; formal analysis, B.D. and T.S.; investigation, B.D. and M.K.; resources, B.D. and T.S.; writing—original draft preparation, B.D. and T.S.; writing—review and editing, B.D. and M.K.; supervision, B.D. and M.K.; project administration, B.D. All authors have read and agreed to the published version of the manuscript.

Funding: This research was funded by COST (European Cooperation in Science and Technology) Action CA16201 PARTICLEFACE and partly by the Polish National Science Center (NCN) under grant 2015/17/N/ST2/04067 and the research activities co-financed by the funds granted under the Research Excellence Initiative of the University of Silesia in Katowice.

Institutional Review Board Statement: Not applicable.

Informed Consent Statement: Not applicable.

Data Availability Statement: Not applicable.

Acknowledgments: We thank Janusz Gluza for useful remarks and discussions.

Conflicts of Interest: The authors declare no conflict of interest.

Abbreviations

The following abbreviations are used in this manuscript:

BSM	Beyond Standard Model
HTM	Higgs Triplet Model
LFV	Lepton Flavour Violation
LNV	Lepton Number Violation
SM	Standard Model
VEV	Vacuum Expectation Value

Appendix A

Appendix A.1. The Scalar Potential of the Model

The scalar potential can be expressed as [49]:

$$\begin{aligned} V &= -m_\Phi^2\left(\Phi^\dagger\Phi\right) + \frac{\lambda}{4}\left(\Phi^\dagger\Phi\right)^2 + M_\Delta^2\,\mathrm{Tr}\left(\Delta^\dagger\Delta\right) + \left[\mu\left(\Phi^T i\sigma_2\Delta^\dagger\Phi\right) + \mathrm{h.c.}\right] \\ &\quad + \lambda_1\left(\Phi^\dagger\Phi\right)\mathrm{Tr}\left(\Delta^\dagger\Delta\right) + \lambda_2\left[\mathrm{Tr}\left(\Delta^\dagger\Delta\right)\right]^2 + \lambda_3\,\mathrm{Tr}\left[\left(\Delta^\dagger\Delta\right)^2\right] + \lambda_4\Phi^\dagger\Delta\Delta^\dagger\Phi\,, \end{aligned} \tag{A1}$$

where Φ indicates SM doublet, μ, λ and λ_i $(i = 1, \ldots, 4)$ are real dimensionless couplings. The m_Φ^2 and M_Δ^2 can be expressed as functions of model parameters together with triplet and doublet VEV's (v_Δ, v_Φ):

$$m_\Phi^2 = \frac{\lambda}{4}v_\Phi^2 + \frac{(\lambda_1+\lambda_4)}{2}v_\Delta^2 - \sqrt{2}\mu\, v_\Delta\,, \tag{A2}$$

$$M_\Delta^2 = -(\lambda_2+\lambda_3)\, v_\Delta^2 - \frac{(\lambda_1+\lambda_4)}{2}v_\Phi^2 + \frac{\mu}{\sqrt{2}}\frac{v_\Phi^2}{v_\Delta}\,. \tag{A3}$$

Physical states are obtained by a rotation of the triplet and doublet fields. Here, we are presenting that dependence in a simplified way:

$$\begin{array}{lcrcrl} h & = & \cos\alpha & h_\phi & + & \sin\alpha \;\; h_\Delta, \\ H & = & -\sin\alpha & h_\phi & + & \cos\alpha \;\; h_\Delta, \\ H^\pm & = & -\sin\beta & w^\pm_\Phi & + & \cos\beta \;\; w^\pm_\Delta, \\ H^{\pm\pm} & = & \delta^{\pm\pm}, & & & \end{array} \tag{A4}$$

where α and β are functions of the scalar potential parameters and multiplets VEV's. The exact formulas can be found in [49] and in the Appendix of [37]. In this paper, only the approximation for $v_\Delta \ll v_\Phi$: $\sin\alpha \;\sim\; 2\frac{v_\Delta}{v_\Phi}$ [53], $\tan\beta = \frac{\sqrt{2}v_\Delta}{v_\Phi}$ is presented. The physical states masses are as follows:

$$\begin{array}{rcl} M_h^2 & = & \lambda v_\Phi^2 \cos^2\alpha + \left(\frac{\mu v_\Phi^2}{\sqrt{2}v_\Delta} + 2v_\Delta^2(\lambda_2+\lambda_3)\right)\sin^2\alpha + 2\Big(v_\Phi v_\Delta(\lambda_1+\lambda_4) - \sqrt{2}\mu v_\Phi\Big)\cos\alpha\sin\alpha, \\ M_H^2 & = & \lambda v_\Phi^2 \sin^2\alpha + \left(\frac{\mu v_\Phi^2}{\sqrt{2}v_\Delta} + 2v_\Delta^2(\lambda_2+\lambda_3)\right)\cos^2\alpha - 2\Big(v_\Phi v_\Delta(\lambda_1+\lambda_4) - \sqrt{2}\mu v_\Phi\Big)\cos\alpha\sin\alpha, \end{array}$$

$$\begin{array}{rcl} M^2_{H^\pm} & = & \frac{(2\sqrt{2}\mu - \lambda_4 v_\Delta)}{4v_\Delta}(v_\Phi^2 + 2v_\Delta^2), \\ M^2_{H^{\pm\pm}} & = & \frac{\mu v_\Phi^2}{\sqrt{2}v_\Delta} - \frac{\lambda_4}{2}v_\Phi^2 - \lambda_3 v_\Delta^2. \end{array} \tag{A5}$$

Appendix A.2. Scalar-Leptons Couplings

Here we present the exact formulas for the $H^{\pm\pm} - l_i - l_j$ and $H^\pm - l_i - \nu_j$ vertices, derived from the Yukawa Lagrangiang for the scalar triplet Δ (see Equation (2)):

$$\mathcal{V}^{\pm\pm} = \begin{cases} l_i^+ - l_j^+ - H^{--} & = & i\left(\mathcal{Y}_{ij} + \mathcal{Y}_{ji}\right), \\ l_i^- - l_j^- - H^{++} & = & i\left(\mathcal{Y}^*_{ij} + \mathcal{Y}^*_{ji}\right), \end{cases} \tag{A6}$$

$$\mathcal{V}^\pm_\Delta = \begin{cases} \tilde{\nu}_i - l_j^+ - H^- = \frac{i}{\sqrt{2}}\cos\beta\left(\mathcal{Y}_{ij} + \mathcal{Y}_{ji}\right), \\ \nu_i - l_j^- - H^+ = \frac{i}{\sqrt{2}}\cos\beta\left(\mathcal{Y}^*_{ij} + \mathcal{Y}^*_{ji}\right), \end{cases} \tag{A7}$$

where $\mathcal{Y}_{ij}$ is the Yukawa coupling, and from the neutrino mass diagonalisation we obtain [37] the following formula. m_{ν_i} means neutrino mass and V_{PMNS} is the Pontecorvo–Maki–Nakagawa–Sakata matrix, parametrised as in the Equation (A9) (s_{ij}, c_{ij} denote $\sin(\theta_{ij})$ / $\cos(\theta_{ij})$).

$$\mathcal{Y}_{ij} = \frac{1}{\sqrt{2}v_\Delta}\, V^*_{PMNS}\, D_\nu\, V^\dagger_{PMNS} \quad , \qquad D_\nu = \mathrm{diag}\{m_{\nu_1}, m_{\nu_2}.m_{\nu_3}\}, \tag{A8}$$

$$V_{\mathrm{PMNS}} = \begin{bmatrix} c_{12}c_{13}e^{i\alpha_1} & s_{12}c_{13}e^{i\alpha_2} & s_{13}e^{-i\delta_{CP}} \\ (-s_{12}c_{23} - c_{12}s_{23}s_{13}e^{i\delta_{CP}})e^{i\alpha_1} & (c_{12}c_{23} - s_{12}s_{23}s_{13}e^{i\delta_{CP}})e^{i\alpha_2} & s_{23}c_{13} \\ (s_{12}s_{23} - c_{12}c_{23}s_{13}e^{i\delta_{CP}})e^{i\alpha_1} & (-c_{12}s_{23} - s_{12}c_{23}s_{13}e^{i\delta_{CP}})e^{i\alpha_2} & c_{23}c_{13} \end{bmatrix}. \tag{A9}$$

Appendix A.3. Feynman Diagrams

Below, we list the most relevant diagrams which contribute to the processes considered in the work, in which one doubly charged Higgs boson is present (so those marked with blue in Table 1). We keep the same numeration as in the mentioned table, so we had chosen the processes (II), (IV), (VII), $(VIII)$ and (IX).

$(II) \quad pp \to H^{\pm\pm}H^{\mp}$

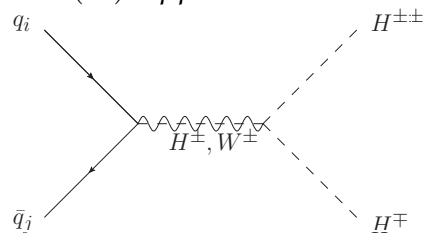

(a)

$(IV) \quad pp \to H^{\pm\pm}ZH^{\mp}$

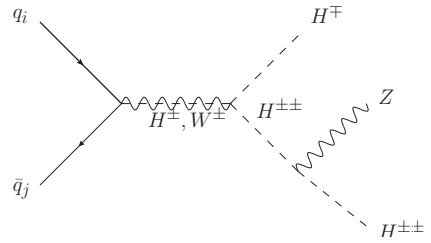

(b)

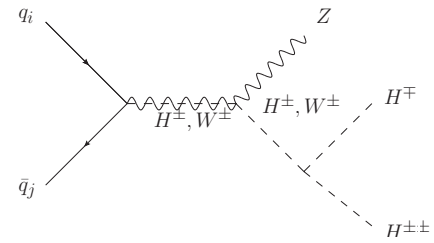

(c)

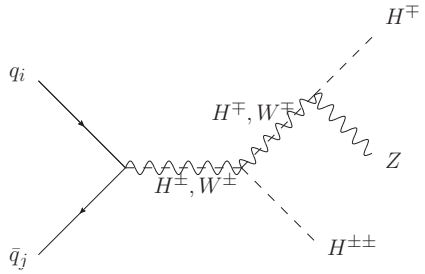

(d)

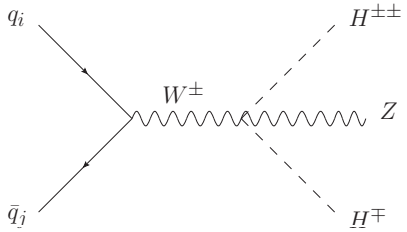

(e)

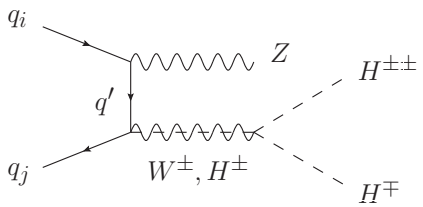

(f)

$(VII) \quad pp \to H^{\pm\pm}W^{\mp}H$

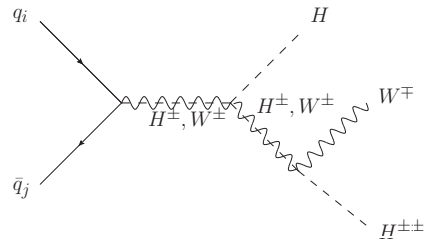

(g)

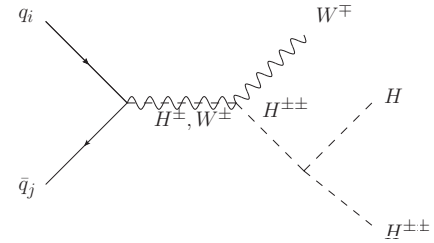

(h)

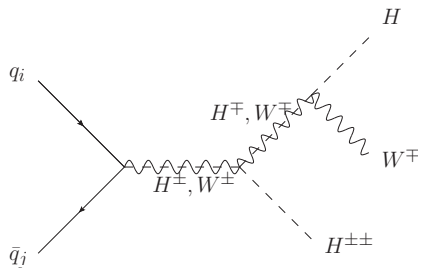

(i)

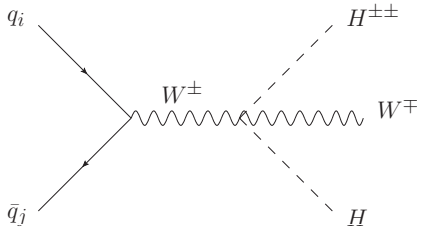

(j)

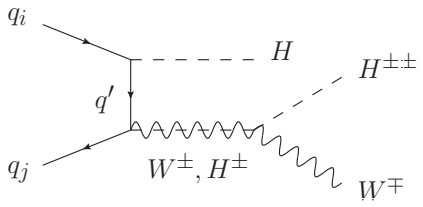

(k)

$(VIII) \quad pp \to H^{\pm\pm}W^{\mp}H^{\mp}$

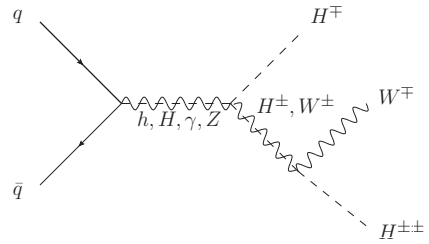

(l)

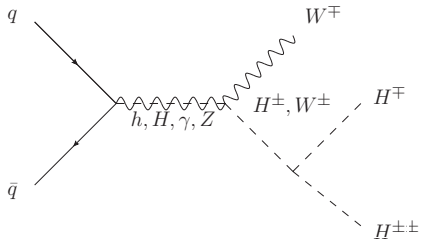

(m)

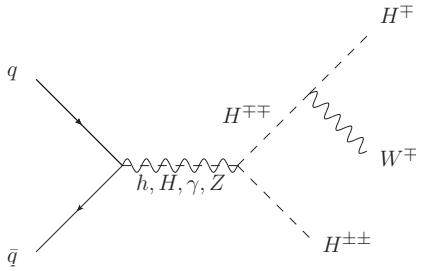

(n)

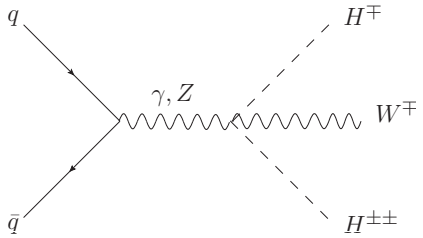

(o)

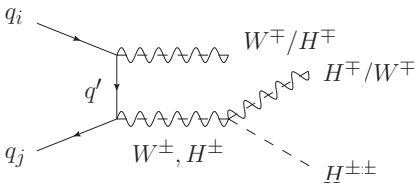

(p)

$(IX) \quad pp \to H^{\pm\pm}hH^{\mp}$

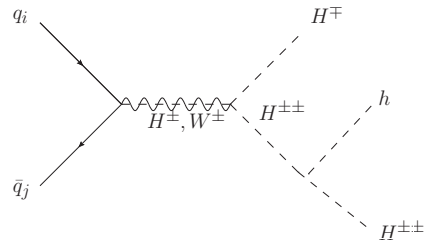

(r)

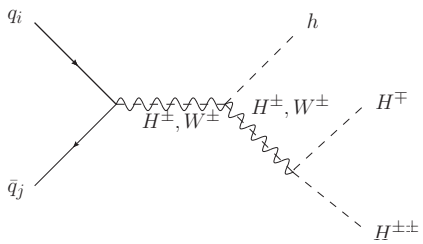

(s)

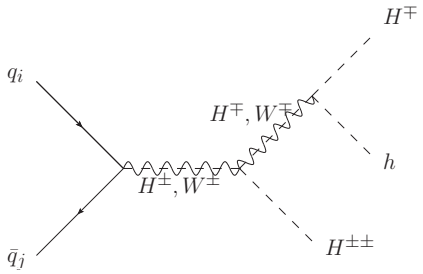

(t)

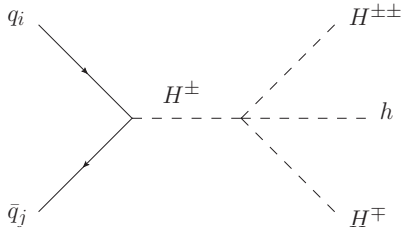

(u)

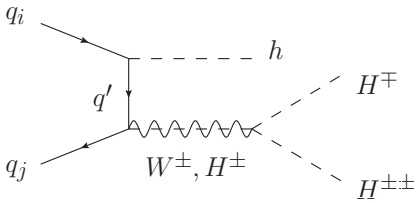

(w)

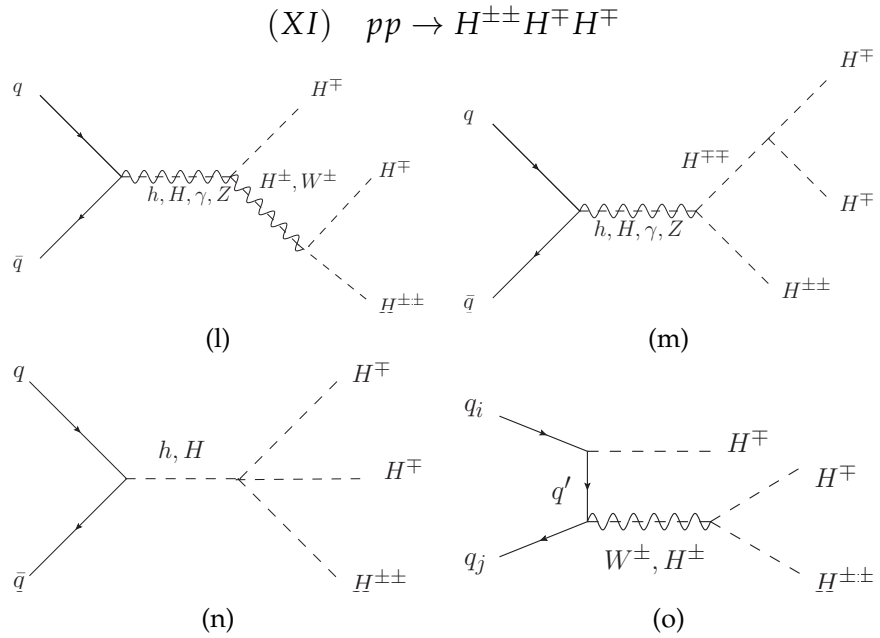

Figure A1. Feynman diagrams for singly and doubly charged scalars production in pp collision, associated with other spin 0 particles (gauge and scalar bosons).

References

1. Aad, G.; Abajyan, T.; Abbott, B.; Abdallah, J.; Khalek, S.A.; Abdelalim, A.A.; Aben, R.; Abi, B.; Abolins, M.; AbouZeid, O.S.; et al. Observation of a new particle in the search for the Standard Model Higgs boson with the ATLAS detector at the LHC. *Phys. Lett.* **2012**, *B716*, 1–29. [CrossRef]
2. Chatrchyan, S.; Khachatryan, V.; Sirunyan, A.M.; Tumasyan, A.; Adam, W.; Aguilo, E.; Bergauer, T.; Dragicevic, M.; Erö, J.; Fabjan, C.; et al. Observation of a New Boson at a Mass of 125 GeV with the CMS Experiment at the LHC. *Phys. Lett.* **2012**, *B716*, 30–61. [CrossRef]
3. Mohapatra, R.N.; Pati, J.C. A Natural Left-Right Symmetry. *Phys. Rev.* **1975**, *D11*, 2558. [CrossRef]
4. Senjanovic, G.; Mohapatra, R.N. Exact Left-Right Symmetry and Spontaneous Violation of Parity. *Phys. Rev.* **1975**, *D12*, 1502. [CrossRef]
5. Mohapatra, R.N.; Senjanović, G. Neutrino Mass and Spontaneous Parity Nonconservation. *Phys. Rev. Lett.* **1980**, *44*, 912–915. [CrossRef]
6. Deshpande, N.G.; Gunion, J.F.; Kayser, B.; Olness, F. Left-right-symmetric electroweak models with triplet Higgs field. *Phys. Rev. D* **1991**, *44*, 837–858. [CrossRef] [PubMed]
7. Duka, P.; Gluza, J.; Zralek, M. Quantization and renormalization of the manifest left-right symmetric model of electroweak interactions. *Ann. Phys.* **2000**, *280*, 336–408. [CrossRef]
8. Barenboim, G.; Gorbahn, M.; Nierste, U.; Raidal, M. Higgs sector of the minimal left-right symmetric model. *Phys. Rev.* **2002**, *D65*, 095003. [CrossRef]
9. Gunion, J.F.; Haber, H.E.; Kane, G.L.; Dawson, S. *The Higgs Hunter's Guide*; CRC Press: Boca Raton, FL, USA, 2000; Volume 80.
10. Chun, E.J.; Lee, K.Y.; Park, S.C. Testing Higgs triplet model and neutrino mass patterns. *Phys. Lett.* **2003**, *B566*, 142–151. [CrossRef]
11. Pati, J.C.; Salam, A. Lepton Number as the Fourth Color. *Phys. Rev. D* **1974**, *10*, 275–289; Erratum in **1975** *11*, 703–703. [CrossRef]
12. Georgi, H.; Machacek, M. Doubly charged Higgs bosons. *Nucl. Phys. B* **1985**, *262*, 463–477. [CrossRef]
13. Gunion, J.F.; Vega, R.; Wudka, J. Higgs triplets in the standard model. *Phys. Rev. D* **1990**, *42*, 1673–1691. [CrossRef] [PubMed]
14. Gunion, J.F.; Grifols, J.; Mendez, A.; Kayser, B.; Olness, F. Higgs bosons in left-right-symmetric models. *Phys. Rev. D* **1989**, *40*, 1546–1561. [CrossRef] [PubMed]
15. Vega, R.; Dicus, D.A. Doubly charged Higgs and W^+W^+ production. *Nucl. Phys. B* **1990**, *329*, 533–546. [CrossRef]
16. Huitu, K.; Maalampi, J.; Pietila, A.; Raidal, M. Doubly charged Higgs at LHC. *Nucl. Phys.* **1997**, *B487*, 27–42. [CrossRef]
17. Barger, V.D.; Baer, H.; Keung, W.Y.; Phillips, R.J.N. Decays of Weak Vector Bosons and T Quarks Into Doubly Charged Higgs Scalars. *Phys. Rev. D* **1982**, *26*, 218. [CrossRef]
18. Muhlleitner, M.; Spira, M. A Note on doubly charged Higgs pair production at hadron colliders. *Phys. Rev. D* **2003**, *68*, 117701. [CrossRef]
19. Primulando, R.; Julio, J.; Uttayarat, P. Scalar phenomenology in type-II seesaw model. *JHEP* **2019**, *8*, 24. [CrossRef]

20. Dutta, B.; Eusebi, R.; Gao, Y.; Ghosh, T.; Kamon, T. Exploring the doubly charged Higgs boson of the left-right symmetric model using vector boson fusionlike events at the LHC. *Phys. Rev. D* **2014**, *90*, 055015. [CrossRef]
21. Bambhaniya, G.; Chakrabortty, J.; Gluza, J.; Jelinski, T.; Szafron, R. Search for doubly charged Higgs bosons through vector boson fusion at the LHC and beyond. *Phys. Rev. D* **2015**, *92*, 015016. [CrossRef]
22. Hessler, A.G.; Ibarra, A.; Molinaro, E.; Vogl, S. Impact of the Higgs boson on the production of exotic particles at the LHC. *Phys. Rev. D* **2015**, *91*, 115004. [CrossRef]
23. Han, T.; Mukhopadhyaya, B.; Si, Z.; Wang, K. Pair production of doubly-charged scalars: Neutrino mass constraints and signals at the LHC. *Phys. Rev. D* **2007**, *76*, 075013. [CrossRef]
24. Drees, M.; Godbole, R.M.; Nowakowski, M.; Rindani, S.D. gamma gamma processes at high-energy p p colliders. *Phys. Rev. D* **1994**, *50*, 2335–2338. [CrossRef] [PubMed]
25. Akeroyd, A.G.; Aoki, M. Single and pair production of doubly charged Higgs bosons at hadron colliders. *Phys. Rev. D* **2005**, *72*, 035011. [CrossRef]
26. Akeroyd, A.G.; Aoki, M.; Sugiyama, H. Probing Majorana Phases and Neutrino Mass Spectrum in the Higgs Triplet Model at the CERN LHC. *Phys. Rev. D* **2008**, *77*, 075010. [CrossRef]
27. Akeroyd, A.G.; Sugiyama, H. Production of doubly charged scalars from the decay of singly charged scalars in the Higgs Triplet Model. *Phys. Rev. D* **2011**, *84*, 035010. [CrossRef]
28. Alloul, A.; Frank, M.; Fuks, B.; Rausch de Traubenberg, M. Doubly-charged particles at the Large Hadron Collider. *Phys. Rev. D* **2013**, *88*, 075004. [CrossRef]
29. Li, T. Type II Seesaw and tau lepton at the HL-LHC, HE-LHC and FCC-hh. *JHEP* **2018**, *9*, 79. [CrossRef]
30. Dev, P.S.B.; Ramsey-Musolf, M.J.; Zhang, Y. Doubly-Charged Scalars in the Type-II Seesaw Mechanism: Fundamental Symmetry Tests and High-Energy Searches. *Phys. Rev.* **2018**, *D98*, 055013. [CrossRef]
31. Crivellin, A.; Ghezzi, M.; Panizzi, L.; Pruna, G.M.; Signer, A. Low- and high-energy phenomenology of a doubly charged scalar. *Phys. Rev. D* **2019**, *99*, 035004. [CrossRef]
32. Du, Y.; Dunbrack, A.; Ramsey-Musolf, M.J.; Yu, J.H. Type-II Seesaw Scalar Triplet Model at a 100 TeV pp Collider: Discovery and Higgs Portal Coupling Determination. *JHEP* **2019**, *1*, 101. [CrossRef]
33. Antusch, S.; Fischer, O.; Hammad, A.; Scherb, C. Low scale type II seesaw: Present constraints and prospects for displaced vertex searches. *JHEP* **2019**, *2*, 157. [CrossRef]
34. de Melo, T.B.; Queiroz, F.S.; Villamizar, Y. Doubly Charged Scalar at the High-Luminosity and High-Energy LHC. *Int. J. Mod. Phys. A* **2019**, *34*, 1950157. [CrossRef]
35. Padhan, R.; Das, D.; Mitra, M.; Kumar Nayak, A. Probing doubly and singly charged Higgs bosons at the pp collider HE-LHC. *Phys. Rev. D* **2020**, *101*, 075050. [CrossRef]
36. Fuks, B.; Nemevsek, M.; Ruiz, R. Doubly Charged Higgs Boson Production at Hadron Colliders. *Phys. Rev. D* **2020**, *101*, 075022. [CrossRef]
37. Gluza, J.; Kordiaczyńska, M.; Srivastava, T. Discriminating the HTM and MLRSM models in collider studies via doubly charged Higgs boson pair production and the subsequent leptonic decays. *Chin. Phys. C* **2021**. accept.
38. Yang, X.H.; Yang, Z.J. Doubly Charged Higgs Production at Future ep Colliders. *arXiv* **2021**, arXiv:2103.11412.
39. Aaboud, M.; Aad, G.; Abbott, B.; Abeloos, B.; Abidi, S.H.; AbouZeid, O.S.; Abraham, N.L.; Abramowicz, H.; Abreu, H.; Abreu, R.; et al. Search for doubly charged Higgs boson production in multi-lepton final states with the ATLAS detector using proton-proton collisions at $\sqrt{s}$ = 13 TeV. *arXiv* **2017**, arXiv:1710.09748.
40. Aad, G.; Abbott, B.; Abbott, D.C.; Abud, A.A.; Abeling, K.; Abhayasinghe, D.K.; Abidi, S.H.; Abouzeid, O.; Abraham, N.; Abramowicz, H.; et al. Search for doubly and singly charged Higgs bosons decaying into vector bosons in multi-lepton final states with the ATLAS detector using proton-proton collisions at $\sqrt{s}$ = 13 TeV. *arXiv* **2021**, arXiv:2101.11961.
41. A Search for Doubly-Charged HIGGS Boson Production in Three and Four Lepton Final States at $\sqrt{s} = 13$ TeV. 2017. Available online: http://cds.cern.ch/record/2242956 (accessed on 2 July 2021).
42. High-Luminosity LHC, CERN. Available online: https://home.cern/science/accelerators/high-luminosity-lhc (accessed on 2 July 2021).
43. Ellis, R.K.; Sozzi, M.; Nisati, A.; D'Onofrio, M.; Siklér, F.; Schulte, D.; D'Hondt, J.; Jaeckel, J.; McCullough, M.; Wiedemann, U.; et al. Physics Briefing Book: Input for the European Strategy for Particle Physics Update 2020. *arXiv* **2019**, arXiv:1910.11775.
44. Contino, R.; Curtin, D.; Katz, A.; Mangano, M.L.; Panico, G.; Ramsey-Musolf, M.J.; Zanderighi, G.; Anastasiou, C.; Astill, W.; Bambhaniya, G.; et al. Physics at a 100 TeV pp collider: Higgs and EW symmetry breaking studies. *CERN Yellow Rep.* **2017**, *3*, 255–440. [CrossRef]
45. Contino, R.; Curtin, D.; Katz, A.; Mangano, M.L.; Panico, G.; Ramsey-Musolf, M.J.; Zanderighi, G.; Anastasiou, C.; Astill, W.; Bambhaniya, G.; et al. Physics at a 100 TeV pp collider: Beyond the Standard Model phenomena. *CERN Yellow Rep.* **2017**, *3*, 441–634. [CrossRef]
46. Abada, A.; Abbrescia, M.; AbdusSalam, S.S.; Abdyukhanov, I.; Fernandez, J.A.; Abramov, A.; Aburaia, M.; Acar, A.O.; Adzic, P.R.; Agrawal, P.; et al. FCC Physics Opportunities. *Eur. Phys. J.* **2019**, *C79*, 474. [CrossRef]
47. FCC Collaboration. FCC-hh: The Hadron Collider: Future Circular Collider Conceptual Design Report Volume 3. *Eur. Phys. J. ST* **2019**, *228*, 755–1107. [CrossRef]

48. FCC—Future Circular Collider, Conceptual Design Report. Available online: https://fcc-cdr.web.cern.ch/ (accessed on 2 July 2021).
49. Arhrib, A.; Benbrik, R.; Chabab, M.; Moultaka, G.; Peyranere, M.C.; Rahili, L.; Ramadan, J. The Higgs Potential in the Type II Seesaw Model. *Phys. Rev.* **2011**, *D84*, 095005. [CrossRef]
50. Akeroyd, A.G.; Moretti, S. Enhancement of H to gamma gamma from doubly charged scalars in the Higgs Triplet Model. *Phys. Rev.* **2012**, *D86*, 035015. [CrossRef]
51. Chun, E.J.; Lee, H.M.; Sharma, P. Vacuum Stability, Perturbativity, EWPD and Higgs-to-diphoton rate in Type II Seesaw Models. *JHEP* **2012**, *11*, 106. [CrossRef]
52. Gluza, J.; Kordiaczyńska, M.; Srivastava, T. Doubly Charged Higgs Bosons and Spontaneous Symmetry Breaking at eV and TeV Scales. *Symmetry* **2020**, *12*, 153. [CrossRef]
53. Das, D.; Santamaria, A. Updated scalar sector constraints in Higgs triplet model. *Phys. Rev.* **2016**, *D94*, 015015. [CrossRef]
54. Cai, Y.; Han, T.; Li, T.; Ruiz, R. Lepton Number Violation: Seesaw Models and Their Collider Tests. *Front. Phys.* **2018**, *6*, 40. [CrossRef]
55. Pumplin, J.; Stump, D.R.; Huston, J.; Lai, H.L.; Nadolsky, P.; Tung, W.K. New generation of parton distributions with uncertainties from global QCD analysis. *JHEP* **2002**, *7*, 12. [CrossRef]
56. Hou, T.J.; Gao, J.; Hobbs, T.J.; Xie, K.; Dulat, S.; Guzzi, M.; Huston, J.; Nadolsky, P.; Pumplin, J.; Schmidt, C.; et al. New CTEQ global analysis of quantum chromodynamics with high-precision data from the LHC. *arXiv* **2019**, arXiv:1912.10053.
57. Alwall, J., Frederix, R., Frixione, S.; Hirschi, V.; Maltoni, F.; Mattelaer, O.; Shao, H.-S.; Stelzer, T.; Torrielli, P.; Zaro, M. The automated computation of tree-level and next-to-leading order differential cross section, and their maching to parton shower simulations. *JHEP* **2014**, *7*, 79. [CrossRef]
58. Sjostrand, T.; Mrenna, S.; Skands, P.Z. A Brief Introduction to PYTHIA 8.1. *Comput. Phys. Commun.* **2008**, *178*, 852–867. [CrossRef]
59. Sjostrand, T.; Mrenna, S.; Skands, P.Z. PYTHIA 6.4 Physics and Manual. *JHEP* **2006**, *5*, 26. [CrossRef]
60. Alloul, A.; Christensen, N.D.; Degrange, C.; Duhr, C.; Fuks, B. FeynRules 2.0—A complete toolbox for tree-level phenomenology. *Comput. Phys. Commun.* **2014**, *185*, 2250–2300. [CrossRef]
61. Gluza, J.; Zralek, M. Feynman rules for Majorana neutrino interactions. *Phys. Rev. D* **1992**, *45*, 1693–1700. [CrossRef] [PubMed]
62. Esteban, I.; Gonzalez-Garcia, M.C.; Hernandez-Cabezudo, A.; Maltoni, M.; Schwetz, T. Global analysis of three-flavour neutrino oscillations: Synergies and tensions in the determination of θ_{23}, δ_{CP}, and the mass ordering. *JHEP* **2019**, *1*, 106. [CrossRef]
63. Chakrabortty, J.; Gluza, J.; Sevillano, R.; Szafron, R. Left-Right Symmetry at LHC and Precise 1-Loop Low Energy Data. *JHEP* **2012**, *7*, 38. [CrossRef]
64. Bambhaniya, G.; Chakrabortty, J.; Gluza, J.; Kordiaczyńska, M.; Szafron, R. Left-Right Symmetry and the Charged Higgs Bosons at the LHC. *JHEP* **2014**, *5*, 33. [CrossRef]
65. Bambhaniya, G.; Chakrabortty, J.; Gluza, J.; Jeliński, T.; Kordiaczynska, M. Lowest limits on the doubly charged Higgs boson masses in the minimal left-right symmetric model. *Phys. Rev.* **2014**, *D90*, 095003. [CrossRef]
66. Chakrabortty, J.; Gluza, J.; Jelinski, T.; Srivastava, T. Theoretical constraints on masses of heavy particles in Left-Right Symmetric Models. *Phys. Lett.* **2016**, *B759*, 361–368. [CrossRef]